Mutagenesis of a Proton Linkage Pathway in *Escherichia coli* Manganese Superoxide Dismutase†

Mei M. Whittaker and James W. Whittaker*

Department of Biochemistry and Molecular Biology, Oregon Graduate Institute of Science and Technology, P.O. Box 91000, Portland, Oregon 97291-1000

Received February 25, 1997; Revised Manuscript Received May 19, 1997⊗

ABSTRACT: Mutagenesis of *Escherichia coli* manganese superoxide dismutase (MnSD) demonstrates involvement of the strictly conserved gateway tyrosine (Y34) in exogenous ligand interactions. Conservative replacement of this residue by phenylalanine (Y34F) affects the pH sensitivity of the active-site metal ion and perturbs ligand binding, stabilizing a temperature-independent six-coordinate azide complex. Mutant complexes characterized by optical and electron paramagnetic resonance (EPR) spectroscopy are distinct from the corresponding wild-type forms and the anion affinities are altered, consistent with modified basicity of the metal ligands. However, dismutase activity is only slightly reduced by mutagenesis, implying that tyrosine-34 is not essential for catalysis and may function indirectly as a proton donor for turnover, coupled to a protonation cycle of the metal ligands. *In vivo* substitution of Fe for Mn in the MnSD wild-type and mutant proteins leads to increased affinity for azide and altered active-site properties, shifting the pH-dependent transition of the active site from 9.7 (Mn) to 6.4 (Fe) for wt enzyme. This pH-coupled transition shifts once more to a higher effective pK_a for Y34F Fe_2-MnSD, allowing the mutant to be catalytically active well into the physiological pH range and decreasing the metal selectivity of the enzyme. Peroxide sensitivities of the Fe complexes are distinct for the wild-type and mutant proteins, indicating a role for Y34 in peroxide interactions. These results provide evidence for a conserved peroxide−protonation linkage pathway in superoxide dismutases, analogous to the proton relay chains of peroxidases, and suggests that the selectivity of Mn and Fe superoxide dismutases is determined by proton coupling with metal ligands.

Antioxidant metalloenzymes, including superoxide dismutases and catalases, defend biological systems against oxidative challenges arising from toxic oxygen metabolites (Fridovich, 1986; Bannister et al., 1987). Superoxide dismutases are ubiquitous metalloenzymes whose redox-active metal cofactor [Mn (Weisiger & Fridovich, 1973), Fe (Yost & Fridovich, 1976), Cu-Zn (McCord & Fridovich, 1969), or Ni (Youn et al., 1996)] catalyzes the one-electron redox cycle required for superoxide disproportionation:

$$2O_2^{\bullet -} + 2H^+ \rightarrow O_2 + H_2O_2 \qquad (1)$$

This radical-scavenging function appears to protect biological macromolecules from oxidative damage, preventing metabolic and genetic disruption (Keyer et al., 1995). The importance of this protective function is demonstrated by the accelerated mutagenesis and loss of viability of superoxide dismutase-deficient organisms exposed to hyperoxic stress (Farr et al., 1986; Carlioz & Touati, 1986; van Loon et al., 1986; Longo et al., 1996). The eukaryotic Mn superoxide dismutase has recently been the focus of studies relating to cancer (Borrello et al., 1993; Bravard et al., 1992) and aging (Nagley et al., 1992) in the growing field of mitochondrial medicine (Schapira, 1993; Luft & Landau, 1995).

Structures have been solved at atomic resolution for three of the four classes of superoxide dismutases (Ludwig et al., 1991; Borgstahl et al., 1992; Wagner et al., 1993; Church et al., 1995; Stoddard et al., 1990a; Roberts et al., 1991), confirming earlier predictions from sequence analysis for the close structural homology between Mn and Fe enzymes (McCord, 1976; Parker et al., 1987; Parker & Blake 1988a,b), and the distinct protein fold of the Cu-Zn enzyme. Mn and Fe are bound in the respective enzymes by equivalent protein residues (three histidines and an asparate) with a ligating solvent molecule (water or hydroxide) completing a regular trigonal bipyramidal coordination polyhedron. Access to the redox-active metal ion is controlled by three gateway residues that are conserved over all known Fe and MnSD sequences: histidine, tryptophan, and tyrosine side chains pack imperfectly, leaving a small funnel through which anions (superoxide, fluoride, azide) can reach the metal ion (Lah et al., 1995). The gateway tyrosine is involved in a conserved hydrogen-bonding chain extending out from the coordinated solvent (Figure 1) that may function as a relay for delivering protons to oxyanion intermediates during turnover. These conserved residues are important targets for mutagenic dissection of the active-site chemistry, allowing their catalytic roles to be defined by precise modifications of the protein structure. In general, modification of noncoordinating residues can be expected to have a less severe effect on the active-site properties than modification of metal ligands, thus allowing more subtle features of catalysis to be explored. Mutagenesis of the gateway tyrosine (Y34) [previously proposed to have a role in proton transfer for superoxide

† Support for this project from the National Institutes of Health (GM 42680) is gratefully acknowledged.

* Corresponding author. Telephone 503-690-1065; FAX 503-690-1464; Email jim@insight.cbs.ogi.edu.

⊗ Abstract published in *Advance ACS Abstracts,* July 1, 1997.

S0006-2960(97)00421-2 CCC: $14.00

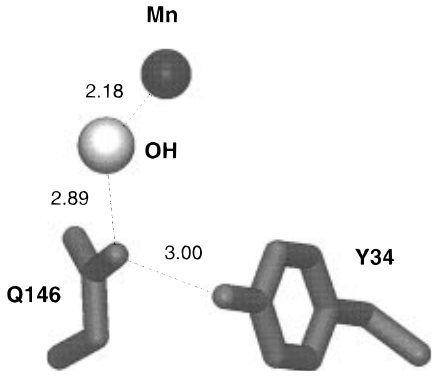

FIGURE 1: Proton linkage pathway in *E. coli* Mn superoxide dismutase. Hydrogen bonding relay chain extending from the aquo cofactor includes glutamine-146 and tyrosine-34 residues [based on a 2.0 Å resolution crystal structure for *E. coli* Mn superoxide dismutase (R. A. Edwards, H. M. Baker, G. B. Jameson, M. M. Whittaker, J. W. Whittaker, E. N. Baker, manuscript in preparation)].

dismutation (Parker & Blake, 1988b; Stoddard et al., 1990a,b; Stallings et al., 1991; Lah et al., 1995)] puts a gap in the gateway and interrupts the conserved H-bonding chain in the active site. The studies reported here examine the chemistry and enzymology of the Y34F gateway mutant.

MATERIALS AND METHODS

E. coli were grown in 2× Luria−Bertani (LB) medium supplemented with 1% glucose, 120 μg/mL ampicillin, and 30 μM Mn(II) or 100 μM Fe(II) salts. Further additions of ampicillin (150 mg/L) were made hourly after the optical density reached 0.3 at 600 nm, and a second addition of 1% glucose was made at mid-log phase. Fermentations for protein preparation were routinely performed in a 10 L New Brunswick Scientific BioFlo 3000 bioreactor. Cultures were grown at 37 °C with vigorous agitation and O_2 purging. Superoxide dismutase was purified as previously described (Whittaker & Whittaker, 1991) with an additional chromatofocusing chromatography step using PBE-94 polybuffer exchanger and Polybuffer-74 ampholyte. Superoxide dismutase activity was measured using the xanthine oxidase/cytochrome *c* inhibition assay (McCord & Fridovich, 1969).

The pDT1-5 antibiotic resistance plasmid containing the sodA locus (Touati, 1983) was a generous gift of Dr. Danièle Touati (Institut Jacques Monod, Centre National de la Récherche Scientifique, Université Paris VII). Plasmids were isolated from overnight cultures with Qiagen Midi Kit and purified according to the protocol supplied by the manufacturer. Mutagenic primers were synthesized by Promega Corp. (Madison, WI). The 34-mers designed to introduce the Y34F mutation (5′-CACCATCAGACCTTCGTAAACAACGCCAACGCGG-3′ and 5′-CCGCGTTGGCGTTGTTTACGAAGGTCTGATGGTG-3′) were gel-purified before use. Mutagenesis of the pDT1-5 plasmid was performed using the Stratagene QuickChange *in vitro* site-directed mutagenesis system with 12 cycles of amplification. PCR products were transformed into Stratagene Epicurian Coli XL-2 ultracompetent *E. coli* cells according to the manufacturer's directions, and transformants were selected on LB agar containing 20 mg/L ampicillin and 80 mg/L methicillin. Mutants were identified using the Promega Silver Sequence DNA sequencing system. A positive clone was selected for expression of the mutant protein and its *sodA* (Y34F) gene was sequenced by the Molecular Biology Core Facility of the Oregon Regional Primate Research Center, Beaverton, OR. High-resolution electrospray mass spectrometry was performed on recombinant MnSD (both wild type and mutant) isolated from high-level expression batch cultures for detailed protein mass analysis (Oregon State University Mass Spectrometry Facility, Environmental Health Sciences Center, Corvallis, OR).

Protein concentration was routinely determined by the method of Lowry (1951) and optical absorption measurements, using the previously reported molar extinction coefficient ($\epsilon_{280} = 8.66 \times 10^4$ M^{-1} cm^{-1}) (Beyer et al., 1989). Metal quantitation was performed by atomic absorption spectrometric analysis using a Varian SpectrAA 20B atomic absorption spectrometer equipped with a GTA-96 graphite furnace for high sensitivity analytical determinations. The purified enzyme was converted to a homogeneous Mn(III) form by molybdicyanide oxidation (Whittaker & Whittaker, 1991). Optical absorption spectra were recorded on a Varian Cary 5 UV−vis−NIR absorption spectrometer interfaced with a PC for data acquisition. EPR spectra were recorded on a Varian E-109 X-band EPR spectrometer equipped with an Air Products He cryostat. Samples of Mn(II) SD[1] for EPR spectroscopy were prepared by dithionite reduction and anaerobic desalting as previously described (Meier et al., 1996).

All reagents for preparation of culture media and buffers were from commercial sources and were used without purification. Ampicillin was obtained from Sigma Chemical Co. Potassium molybdicyanide was prepared as previously described. (Whittaker & Whittaker, 1996).

RESULTS

The recombinant Y34F mutant MnSD is isolated from *E. coli* cells as a purple Mn(III) complex with an optical spectrum (Figure 2) nearly indistinguishable from that of the wild-type MnSD and only slightly reduced catalytic activity (Table 1), the wt MnSD exhibiting a specific activity approximately 20% higher than the mutant. The minor change in the optical spectrum of the Y34F mutant ($\epsilon_{478} =$ 780 M^{-1} (active sites) cm^{-1}) compared to the wt enzyme ($\epsilon_{478} = 850$ M^{-1} (active sites) cm^{-1}) reflects the relatively small perturbation of the metal center expected for modification of a noncoordinating active-site residue. For both wt and mutant MnSD, the catalytic activity shows a weak pH dependence between pH 7.8 and 9 with no differentiation between the two proteins over this range. The site of the mutation has been confirmed by gene sequence analysis identifying the mutagenically introduced A → T transition as the unique site of modification. The mutant protein has also been examined using positive ion electrospray mass spectrometry, which demonstrated an approximately 16 unit mass difference between wild-type protein ($M = 22\,964 \pm 4$) and the Y34F mutant ($M = 22\,950 \pm 4$) consistent with the replacement of a single tyrosine by phenylalanine in the protein structure.

Although there are close similarities between wild-type and mutant proteins, there are several important differences. The Mn(III) absorption spectrum of wt MnSD is relatively

[1] Abbreviations: SD, superoxide dismutase; LMCT, ligand-to-metal charge transfer; EPR, electron paramagnetic resonance.

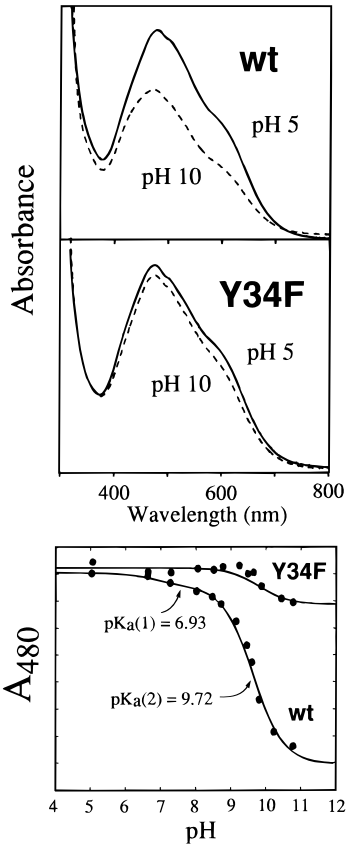

FIGURE 2: Protonation equilibria of Mn superoxide dismutase. (Top) pH-dependent optical spectra for wt MnSD (0.25 mM active sites): (—) in 100 mM potassium acetate buffer, pH 5; (- - -) in 100 mM CAPS-KOH buffer, pH 10. (Middle) pH-dependent optical spectra for Y34F mutant MnSD (0.2 mM active sites): (—) in 100 mM potassium acetate buffer, pH 5; (- - -) in 100 mM CAPS-KOH buffer, pH 10. (Bottom) Optically detected pH titration of wt and mutant MnSD in 100 mM buffer adjusted to ionic strength $\mu = 1$ with Na_2SO_4. pH 5.0, potassium acetate; pH 6.6 and 7.3, $KHPO_4$; pH 8.0, 8.5, and 8.7, Bicine-KOH; pH 9.2, 9.5, and 9.6, CAPSO-KOH; pH 9.8, 10.2, and 10.8, CAPS-KOH. The pH titration profile was fit by regression analysis.

Table 1: Catalytic Activity for MnSD Complexes

MnSD form	SD activity[a] (units/mg)			
	pH 6.3	pH 7.0	pH 7.8	pH 9.0
wt Mn_2-MnSD			7300	5900
Y34F Mn_2-MnSD			6000	5000
wt Fe_2-MnSD	480	140	60	<5
Y34F Fe_2-MnSD	1560	1540	850	150

[a] The average error in these values based on multiple determinations is approximately 10% of the measured value.

sensitive to pH, converting to a form with 33% lower intensity (A_{480}) at pH 10 (Figure 2, top), while under the same conditions the spectrum of the Y34F mutant is essentially unchanged, decreasing only about 6% in intensity (Figure 2, middle). These changes in the optical spectra allow the active-site Mn(III) to be used as a probe of local structural changes in the protein that are communicated to the metal ion via the directly coordinated metal ligands. Analysis of the detailed pH titration profile for wt MnSD (Figure 2, bottom) resolves two inflection points (at pH 6.93 and 9.72). The lower pH transition is close to the expected pK_a for histidine imidazole (p$K_a \sim 7$) in proteins and can be tentatively assigned to ionization of a histidine side chain. The transition at higher pH represents a more dramatic

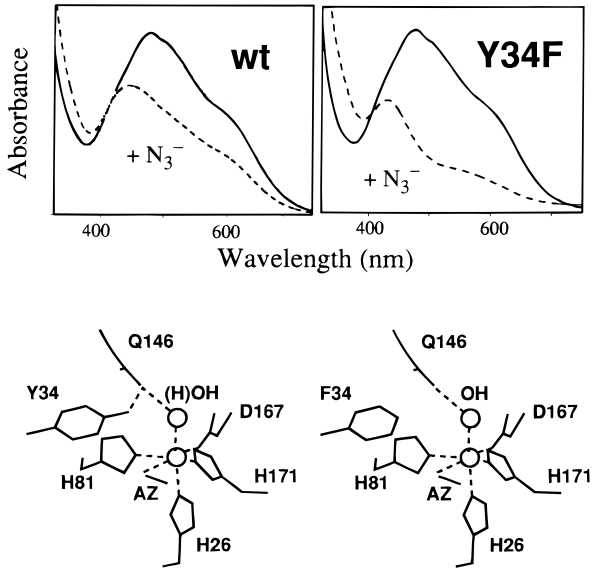

FIGURE 3: Azide interactions in Mn superoxide dismutase complexes. (Top) Optical absorption spectra for wt MnSD (left) and Y34F mutant MnSD (right) native enzyme (0.5 mM active sites) (—) and azide adduct (50 mM NaN_3) (- - -). (Bottom) Structural models for involvement of tyrosine-34 in exogenous ligand binding to the active-site Mn(III) ion.

perturbation of the Mn(III) ion, forming a complex whose optical spectrum resembles that previously found for the fluoride adduct (Whittaker & Whittaker, 1991). On the basis of the optical spectrum (Figure 2, top), the Mn ion remains five-coordinate in this complex. In the Y34F mutant (Figure 2, middle) the titration has a much smaller amplitude and only the higher pH transition is present, possibly associated with ionization of the 6−7 tyrosine residues within approximately 12 Å of the Mn center. The dramatic reduction in amplitude for the high-pH transition in the Y34F mutant suggests a special role for Y34 in the coordination chemistry of the Mn site that is not immediately obvious in the catalytic rate data (Table 1).

These alterations in active-site pH-dependent equilibria in the Y34F mutant have dramatic consequences in anion binding to the Mn(III) protein. The wt MnSD is known to form a five-coordinated azide complex at ambient temperature with a characteristic optical spectrum in which all four spin-allowed ligand field transitions for the high-spin Mn(III) ion lie below 1000 nm (Figure 3, left) (Dingle, 1962, 1965, 1966; Whittaker & Whittaker, 1991, 1996). At low temperature, this complex converts to a six-coordinate form characterized by a splitting of the ligand field spectra that resolves the d → d bands in the visible spectrum and leads to a shift of the lowest-energy absorption band into the near IR, associated with an overall decrease in intensity for the optical spectrum. The spectrum of the azide complex of the Y34F MnSD mutant (Figure 3, right) closely resembles that found for the low-temperature six-coordinate wt MnSD azide complex but does not show any signs of temperature dependence on warming. This spectrum also resembles that reported for a dead-end peroxide-bound intermediate formed during turnover of the *Thermus thermophilus* MnSD in transient kinetics experiments (Bull et al., 1991).

The interactions of other anions with the Mn(III) ion in the oxidized active site are also perturbed by Y34F mutagenesis as reflected in ligand affinities (Table 2) and in the optical spectra of the anion complexes (Figure 4).

Table 2: Anion Affinities for MnSD Complexes

anion	MnSD form	pH	K_D (mM)
N_3^-	wt Mn_2-MnSD	7.0	7.2
	Y34F Mn_2-MnSD	7.0	1.6
	wt Fe_2-MnSD	7.8	0.3
		5.0	0.015
	Y34F Fe_2-MnSD	9.0	0.1
		5.0	0.010
OCN^-	wt Mn_2-MnSD	7.0	13
	Y34F Mn_2-MnSD	7.0	11
F^-	wt Mn_2-MnSD	7.0	25
	Y34F Mn_2-MnSD	7.0	75

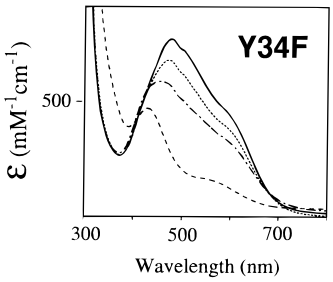

FIGURE 4: Anion complexes of Y34F mutant MnSD. Optical absorption spectra for native Y34F mutant MnSD (0.5 mM active sites) in 50 mM $KHPO_4$ buffer, pH 7.0 (—), in the presence of 1.25 M KF (···), 150 mM KOCN (- · -), or 50 mM NaN_3 (- - -).

Cyanate (OCN^-), like azide, can serve as an electronic analog of the hydroperoxide anion in coordination chemistry. Parallel complexation experiments on wt and mutant MnSD show that cyanate binds to both enzymes with essentially identical affinity (Table 2). The limiting spectrum for the cyanate adduct of the Y34F mutant (Figure 4) reflects predominantly five-coordination of the metal center, in contrast to the six-coordinate complex formed with azide. Since cyanate and azide are both triatomic anions with nearly identical steric requirements, the different protein interactions may be accounted for by their distinct charge distributions. Fluoride affinity for the mutant is lower than for wt MnSD and the optical spectrum is relatively unperturbed, reflecting relatively weak interactions in a complex and that is predicted to be five-coordinate on the basis of its optical spectrum.

EPR spectra shown in Figure 5 provide a comparison between wt and mutant MnSD anion complexes in the reduced [Mn(II)[enzyme. All three anions (F^-, OCN^-, and N_3^-) perturb the Mn(II) sites in both proteins, indicating complex formation. Addition of cyanate and azide results in an increase in the low-field EPR absorption below 500 G (Figure 5C,D). However, azide perturbations of the EPR spectrum of the Y34F MnSD mutant are less pronounced than those found for the wt protein.

Cultivating *E. coli* in medium supplemented with ferrous salts results in substitution of Fe for Mn in the active site of the MnSD protein, reflecting relatively indiscriminant uptake of either Mn or Fe by the protein. The Fe_2-MnSD, a minority species under normal growth conditions (Beyer & Fridovich, 1991), becomes the majority form when excess iron is added to the growth medium. Fe_2-MnSD is formed together with the (Mn,Fe)-MnSD hybrid and the normal Mn_2-MnSD species, which can be separated chromatographically on the basis of subtle charge differences between these species. The optical spectrum of the Fe derivative resembles authentic FeSD (Slykehouse & Fee, 1976) at pH 5, with a strong near-

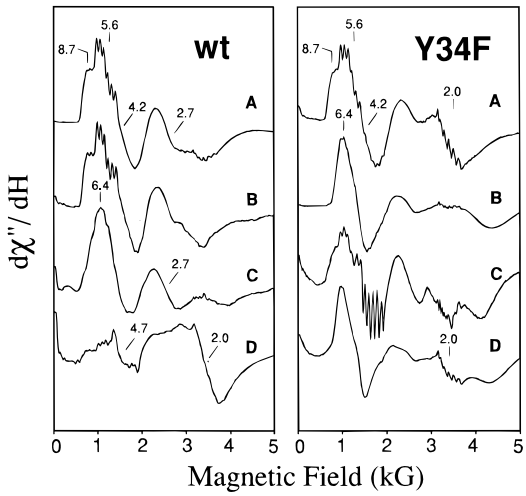

FIGURE 5: X-band EPR spectra for Mn_2-MnSD complexes. (Left) wt MnSD (2.2 mM active sites in 50 mM $KHPO_4$, pH 7). (A) Native enzyme; (B) with 150 mM KOCN; (C) with 400 mM KF (D) with 80 mM NaN_3. (Right) Y34F mutant (2.0 mM active sites in 50 mM $KHPO_4$, pH 7). (A) Native enzyme; (B) with 150 mM KOCN; (C) with 1 M KF; (D) with 25 mM NaN_3. Instrumental parameters: microwave frequency, 9.417 GHz; microwave power, 2.0 mW; modulation amplitude, 10 G; temperature, 5 K.

UV absorption band characteristic of the ferric complex (ϵ_{350} = 1450 M^{-1} cm^{-1}) that bleaches above pH 6 (Figure 6) as the enzyme converts to a distinct form. This transition has been observed for *in vitro* Fe-substituted MnSD from *E. coli* (Yamakura et al., 1994) and other sources (Yamakura et al., 1995). Azide binds to both low- and high-pH forms of Fe_2-MnSD, converting to a unique complex exhibiting a strong azide-to-Fe(III) ligand-to-metal charge transfer (LMCT) absorption near 400 nm (ϵ_{390} = 1700 M^{-1} cm^{-1}). The corresponding derivative of the Y34F mutant has similar spectra (Figure 6). The pH dependence of the optical spectra of wt and Y34F Fe complexes shows that the proton-coupled transition in the mutant protein is shifted 1.5 pH units higher than the corresponding transition in wt Fe_2-MnSD. Superoxide dismutase activity tracks the optical transition, implying that the high-pH form lacks significant SD activity while the low-pH forms of both wt and mutant proteins are competent for catalysis. The specific activity of the Fe derivative of the Y34F mutant at the midpoint of this transition (pH 7.9) is about twice that of the Fe derivative of the wt protein in the same state (pH 6.4) (Table 1). The azide affinities of these complexes are also quite distinct (Table 2). The Fe complexes all show a high affinity for azide, with highest affinity in the catalytically active low-pH form, and the Y34F mutant protein binds the anion more tightly than the wt protein in the corresponding form.

A comparison of ferric Fe_2-MnSD complexes by EPR spectroscopy is shown in Figure 7. EPR spectra recorded for low-pH forms of both wt and mutant complexes reflect a moderately rhombic (E/D = 0.2) environment for the metal ion in the protein. At high pH the metal center converts to a form with a stronger axial perturbation reflected in the EPR spectra (E/D = 0.1) that resemble spectra reported for the authentic *E. coli* FeSD fluoride complex (Slykehouse & Fee, 1976). Azide binding at both low and high pH convert wt and mutant enzymes to a distinct form with nearly identical EPR and optical spectra, reflecting a rhombic limit (E/D = 0.3) to the electronic symmetry in these complexes, quite

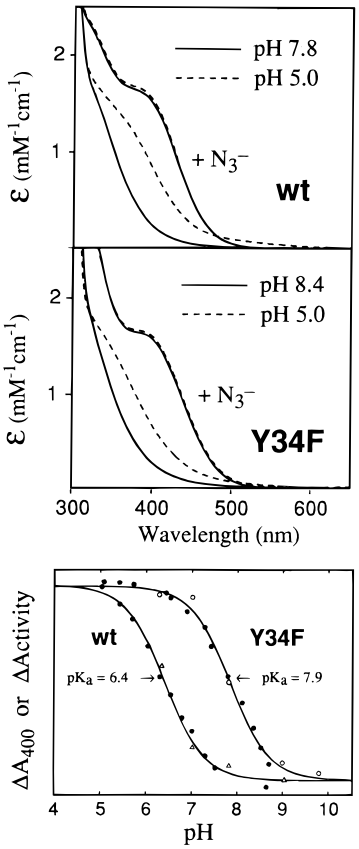

FIGURE 6: Iron-substituted Mn superoxide dismutase. Near-UV optical absorption spectra for Fe_2-MnSD prepared by *in vivo* metallation of the wt MnSD protein (Top) (0.5 mM active sites, in 50 mM $KHPO_4$ buffer) at pH 5.0 (- - -) and pH 7.8 (—) in the absence and presence of 12.5 mM NaN_3. (Middle) Fe_2-MnSD Y34F mutant (0.5 mM active sites, in 50 mM $KHPO_4$ buffer) at pH 5.0 (- - -) and pH 8.4 (—) in the absence and presence of 12.5 mM NaN_3. (Bottom) Optically detected pH titrations for Fe-substituted wt and Y34F mutant MnSD protein prepared by *in vivo* metallation. (●) Normalized spectral profile for 400 nm absorbance; (○) normalized superoxide dismutase activity for Fe_2-MnSD Y34F mutant: (△) normalized superoxide dismutase activity for wt Fe_2-MnSD. Spectroscopic samples approximately 0.35 mM active sites in 100 mM $KHPO_4$ buffer.

different from the azide complex of authentic *E. coli* FeSD (Slykehouse & Fee, 1976), which is known from crystallographic studies to have an azide geometry distinct from that found for MnSD (Lah et al., 1995; Stoddard et al., 1990b).

The sensitivity of the MnSD complexes to hydrogen peroxide is examined in Figure 8. As has been previously reported, wt MnSD is unaffected by exposure to the same moderate levels of H_2O_2 that can inactivate FeSD through oxidation of amino acid side chains (Beyer & Fridovich, 1987). Like its wt counterpart, Mn-containing Y34F mutant is resistant to peroxide, catalytic activity being unchanged after 1 day of incubation with 5 mM H_2O_2 (data not shown). In contrast, under the same conditions, the wt Fe_2-MnSD is 50% inactivated after 34 min. The Y34F Fe_2-MnSD is even more sensitive to peroxide oxidation, being half-inactivated after only 10 min. Increasing the pH increases the peroxide sensitivity even further, leading to half-inactivation of the mutant enzyme in less than 4 min. The inactivation reactions follow single-exponential decay kinetics as shown in the semilog plot (Figure 8).

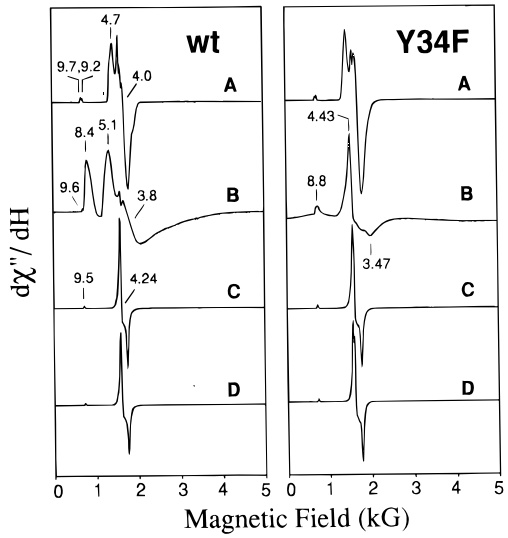

FIGURE 7: X-band EPR spectra for Fe_2-MnSD complexes. (Left) wt Fe_2-MnSD (2 mM active sites) in 50 mM $KHPO_4$ buffer, pH 5.0 (A, C) or pH 7.8 (B, D), in the absence (A, B) or presence (C, D) of 12.5 mM NaN_3. (Right) Fe_2-MnSD Y34F mutant (2 mM active sites) in 50 mM $KHPO_4$ buffer, pH 5.0 (A, C) or pH 7.8 (B, D), in the absence (A, B) or presence (C, D) of 12.5 mM NaN_3. Instrumental parameters: microwave frequency, 9.417 GHz; microwave power, 2.0 mW; modulation amplitude, 10 G; temperature, 5 K.

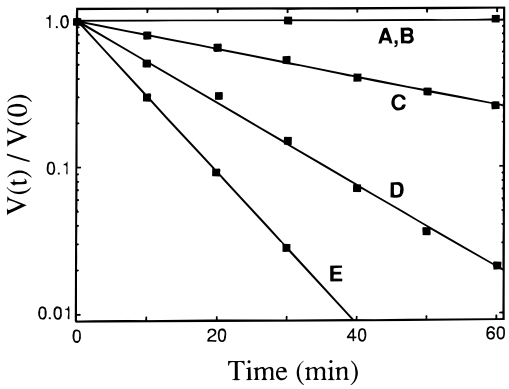

FIGURE 8: Hydrogen peroxide inactivation of MnSD metalloforms. MnSD species [20 μM active sites in 50 mM $KHPO_4$ (pH 7) or $Na_4P_2O_7$ (pH 9)] were incubated with 5 mM H_2O_2 and the reaction was quenched by addition of 10 units of beef liver catalase/μL of reaction mixture. The remaining superoxide dismutase activity [$V(t)$] was measured by xanthine oxidase/cytochrome *c* inhibition assay. (A, B) wt and Y34F Mn_2-MnSD, pH 7.0; (C) wt Fe_2-MnSD, pH 7.0; (D) Y34F Fe_2-MnSD, pH 7.0; (E) Y34F Fe_2-MnSD, pH 9.0.

DISCUSSION

Protons are important in redox catalysis, compensating for the shifts in electronic charge, stabilizing intermediates formed by electron transfer, and assisting in the release of products. The net disproportionation chemistry of the superoxide dismutase redox cycle involves two protons (eq 1) in two distinct half reactions (eqs 2 and 3). The two protons appear unsymmetrically in the equations for these two half reactions, both protons being required in the same (reductive) phase of turnover:

$$\text{OX:} \qquad O_2^{\bullet -} \rightarrow O_2 + 1e^- \tag{2}$$

$$\text{RED:} \qquad O_2^{\bullet -} + 1e^- + 2H^+ \rightarrow H_2O_2 \tag{3}$$

This asymmetry in protons is a consequence of the acidity

of the hydroperoxyl radical [$HO_2^{\bullet}$, pK_a = 4.78 (Sawyer & Valentine, 1981)] that results in ionization of the substrate to the superoxide radical anion at any pH above 5. On the other hand, the protons of H_2O_2 ionize at a relatively high pH [pK_a(1) = 11.6 (Everett & Minkoff, 1953)] and release of product peroxide will involve protonation of the peroxyanion. Efficient operation of the active-site redox engine therefore requires that two donors must be available to deliver these protons at the appropriate point during turnover.

Detailed crystal structures now available for a number of homologous Mn and Fe superoxide dismutases (Ludwig et al., 1991; Borgstahl et al., 1992; Wagner et al., 1993; Stoddard et al., 1990a; Roberts et al., 1991; Lah et al., 1995) suggest a number of possibilities for these proton donors among conserved residues identified by sequence alignments (McCord, 1976; Parker et al., 1987; Parker & Blake, 1988a). The gateway tyrosine Y34 (Figure 1) is an obvious candidate previously proposed to be involved either directly or indirectly in proton transfer events also involving the ligated solvent (Parker & Blake, 1988b; Stoddard et al., 1990a; Stallings et al., 1991; Lah et al., 1995). This solvent molecule undergoes a protonation cycle during turnover, interconverting between hydroxo and aquo forms with the oxidation state of the metal ion, coupling proton uptake with redox (Bull et al., 1991):

$$\text{Mn(III)-OH} + 1e^- + 1H^+ \rightarrow \text{Mn(II)-OH}_2 \qquad (4)$$

This coupling is based on the dramatic shift in acidity between Mn(II) and Mn(III) aqua ions. Water coordinated to divalent Mn is a relatively weak acid (pK_a = 9.82) compared to water bound to Mn(III) (pK_a = 0.2) (Baes & Messmer, 1986). The 10 unit shift in pK_a of a Mn aquo ion between divalent and trivalent oxidation levels provides a driving force for proton transfer to the reduced product (peroxide dianion). In this capacity the ligated solvent may serve as a specialized inorganic cofactor responsible for proton storage and delivery during turnover.

The present mutagenesis experiments conclusively show that tyrosine-34 is *not* essential for turnover and so is unlikely to be directly involved in product formation. However, Y34F mutagenesis does significantly affect turnover and perturbs anion interactions with the active site, suggesting a role for Y34 in product protonation steps. In this role the tyrosine might function in concert with other groups in the protein (viz., Q146 and the ligated solvent) to deliver one of the two catalytic protons through a hydrogen-bond proton relay. Conserved hydrogen-bonding pathways are well-known in other enzymes, including hydrolases [the Ser-His-Asp catalytic triad mechanism for nucleophile stabilization in serine proteases (Carter & Wells, 1988)] and peroxidases [where a His-Asn relay is involved in peroxide deprotonation chemistry in the distal heme pocket (Satterlee et al., 1994; Nagano et al., 1995, 1996) and an Asp-His-Fe triad in the proximal pocket has been implicated in control of metal redox and reactivity (Goodin & McRee, 1993)]. The relay chain motif allows developing charge generated during proton transfer to be stabilized by distribution over an extended donor/acceptor network.

A role for Y34 in the active-site proton circuit is reflected in effects of MnSD mutagenesis on coordination chemistry of the active-site metal ion. Ligand binding to MnSD has recently been shown to result in formation of a five-coordinate complex at physiological temperatures that converts at cryogenic temperatures to a more stable six-coordinate form (Whittaker & Whittaker, 1996). The dynamical instability of the six-coordinate complex appears to result in dissociation of one of the metal ligands, either the ligated solvent or the carboxylate, as the temperature is raised (Whittaker, 1997). These two alternatives are illustrated in Figure 9 in the context of the Y34 proton relay. Five-coordination may result from protonation of the coordinated hydroxide and desolvation (Figure 9A) or from further transfer of a proton and tautomerization of the carboxylate (Figure 9B), which joins with the solvent and Mn ion in forming a six-membered donor/acceptor ring. Conservation of net charge on the buried metal complex requires displacement of one of these anionic ligands (hydroxide or carboxylate) from the metal complex when exogenous anions bind. Shifting a proton along the relay chain facilitates this charge compensation and therefore serves to stabilize anion complexes. Both structures (Figure 9A,B) account for the observed results. Desolvation, which frequently occurs in inorganic complexes that are stable in lower coordination numbers, would lead to the active-site structure shown in Figure 9A. However, crystallographic data for Fe and MnSD azide complexes (interpreted as six-coordinate species) indicates that the largest changes in structure do not involve the coordinated solvent. For FeSD, the equatorial His−Fe−His angle opens (from 132° to 162°) and the Fe shifts 0.2 Å on formation of the azide complex, and for MnSD an elongation of the metal carboxylate vector (by 0.45 Å) in the azide adduct is observed (Lah et al., 1995), both appearing to favor displacement of carboxylate (Figure 9B). The functional significance of this process may be to facilitate peroxide release during turnover through rebinding of the displaced ligand to the metal ion (Whittaker & Whittaker, 1996).

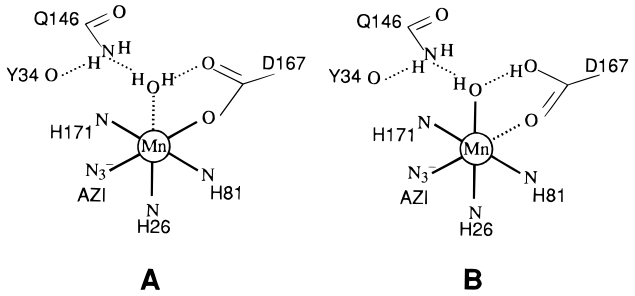

FIGURE 9: Ligand displacement reactions of the active-site Mn complex. Proton transfer along the relay pathway can stabilize either the desolvated complex by protonation of the bound hydroxide (A) or displacement of the bound carboxylate with tautomerization (B), leading to five-coordination in each case.

The azide adduct of MnSD may serve as a model for the transient peroxyanion complex formed during turnover. The stabilizing effect of Y34F mutagenesis on the six-coordinate azide complex indicates that the gateway tyrosine-34 may be important in labilizing the peroxide product complex of superoxide dismutase. The absence of the phenolic donor in the Y34F mutant apparently increases the Lewis basicity of the metal ligands in the proton relay pathway, resulting in a six-coordinate adduct being formed (Figure 3, bottom). Substituting Fe for Mn in a complex will result in a significant perturbation of the metal ligands as illustrated by the distinct pK_a's of Fe(III) and Mn(III) aqua ions in solution (3 versus 0.2) (Baes & Messmer, 1986)]. In MnSD,

Scheme 1

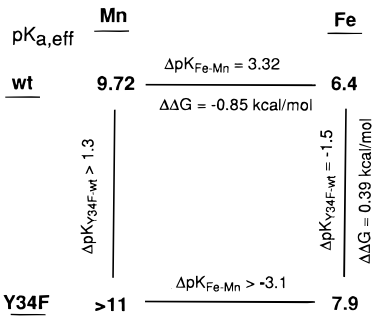

metal substitution will affect all equilibria coupled to ligand protonation along the linkage pathway. The relatively easy protonation of ligands bound to Fe(III) will tend to stabilize exogenous anion complexes through the displacement mechanism. Thus, azide binds to the low-pH form of both wt and mutant Fe_2-MnSD with extremely high affinity, characterized by dissociation constants in the micromolar range. Fe_2-MnSD complexes also hydrolyze in the neutral pH range [pK_a = 6.4 (wt) and 7.9 (Y34F)] binding hydroxide at a vacant coordination site on Fe(III) as proposed for the authentic FeSD from *E. coli* (Tierney et al., 1995) and modeled in the crystal structure for the Fe-containing enzyme from *Propionibacterium shermanii* (Schmidt et al., 1996). The corresponding pH-dependent transition in the wt Mn_2-MnSD (Figure 2) at pH 9.72 can also be interpreted as hydroxide binding by analogy to the results for FeSD. However, the optical spectra show unambiguously that the high-pH (bleached) form of the Mn enzyme is five-coordinate at ambient temperatures, not six-coordinate as is observed for the Fe complexes in low-temperature X-ray absorption studies (Tierney et al., 1995). However, the coordination number of the corresponding Fe complex is unknown at ambient temperature, and it is possible that the structure of the hydroxide adduct is temperature-dependent as has been previously found for the azide and fluoride complexes of MnSD (Whittaker & Whittaker, 1996). There is no obstacle to binding small anions to Mn in the Y34F mutant (Figure 4), so the absence of hydrolysis for Y34F MnSD below pH 11 may be accounted for by a shift of the transition 2 units to higher pH, in analogy with the Fe-substituted MnSD (Figure 6). Correlation between the Fe and Mn complexes of *E. coli* MnSD thus rules out assignment of the pH-linked transition in these complexes to a simple ionization of Y34 as previously proposed on the basis of the similarity of the effective pK_a of the transition in the wt protein to the pK_a expected for tyrosine (Hsu et al., 1996).

These results can be interpreted in terms of coupled equilibria within the active site involving both protein and metal ion contributions as shown in Scheme 1. The shift in effective pK_a for the pH-linked transition in the SD active site between Mn(III) and Fe(III) forms is $\Delta pK = 3.32$, a net stabilization of the hydrolyzed metal complex ($\Delta\Delta G = -0.8$ kcal/mol) resulting from interchange of the metal ions. Changing the protein by Y34F mutagenesis also perturbs the active-site equilibria but in the reverse direction, destabilizing the hydroxide complex (and therefore stabilizing the active form) by approximately 0.3 kcal/mol as reflected in the $\Delta pK = 1.5$ shift in the hydrolysis reaction. Azide binding affinities for the low-pH (catalytically active) forms of Fe_2-MnSD and Mn_2-MnSD also correlate with these data, with $K_D(N_3^-)$ favoring the Fe complex by 3 log units. In addition to affecting ligand interactions, these coupled equilibria are expected to be involved in the redox chemistry of the active-site metal ion.

EPR spectroscopy can provide information on the coordination chemistry of the reduced Mn(II) site, which lacks obvious optical absorption features in the visible region (Figure 5). Perturbation of the high-spin $S = {}^5/_2$ ground state is observed in the presence of anions (F^-, OCN^-, N_3^-) for both wt and mutant proteins. Low-field absorption in these spectra (below 500 G) arises from interdoublet transitions in the spin sextet electronic ground state and reflects small zero-field splitting (D). Interdoublet transitions will occur if $D \approx h\nu$, the microwave photon energy, which at X-band is approximately 0.3 cm^{-1}. For ground states with larger D, the EPR spectra are a superposition of transitions arising within each of the three Kramers doublets associated with large effective g-values between 2 and 10, while for smaller values of D the spectra collapse around the free electron g-value ($g = 2$) (Whittaker & Whittaker, 1991). Inspection of the spectra of the Mn(II)SD anion complexes (Figure 5) indicates that the largest D is associated with the native enzyme and the smallest with the azide adduct. The magnitude of the zero-field splitting correlates with deviations from cubic symmetry, so the qualitative ordering $D_{native} \sim D_{cyanate} > D_{fluoride} > D_{azide}$ suggests that the reduced native Mn(II) protein is five-coordinate while the azide complex, like its Mn(III) counterpart, is six-coordinate at low temperature. Although anions perturb the metal center in the Y34F mutant, change in coordination number is not clearly reflected in the Mn(II) EPR spectra and the complexes appear to remain five-coordinate in this case.

The Fe(III) state of the Fe-substituted MnSD (Figure 7) is isoelectronic with Mn(II), allowing comparison of ligand interactions in reduced Mn and oxidized Fe complexes. The EPR spectra of the ferric protein are characteristic of complexes with large zero-field splitting ($D > h\nu$) typical of high-spin Fe(III) ions (Griffith, 1964). For this d^5 metal ion, transitions in the middle Kramers doublet ($M_S = \pm{}^3/_2$) occur near $g = 4.3$ in the rhombic limit and diverge from that value with increasing axial character, while the $M_S = \pm{}^1/_2$ doublet gives rise to transitions near $g = 6$ and 2 in the axial limit. Hydrolysis of the complex is detected by the pH dependence of the EPR spectra. The low pH spectrum (Figure 7A) is rhombic ($g = 4.7$, 4.0, 3.9 arising within the $M_S = \pm{}^3/_2$ doublet, $E/D \sim 0.2$), converting to a relatively axial spectrum ($g = 8.4$ and 3.8 arising within the $M_S = \pm{}^1/_2$ doublet, $E/D \sim 0.1$) above the transition for the wt protein, whereas the Y34F mutant complex remains rhombic at high pH. Addition of azide converts high- and low-pH forms of both proteins to a unique complex (Figure 7C,D) at the rhombic limit of electronic symmetry. Increasing rhombicity is associated with near-octahedral geometry and six-coordination for Fe(III) since the small departures from exact cubic symmetry are all of similar magnitude, resulting in an effective low symmetry for the site. In contrast, lower coordination results in more axial character, associated with a dominant strong (or weak) perturbation in the complex. The rhombic character observed for the azide adducts of Fe_2-MnSD is thus consistent with six-coordination of these complexes at low temperature, as found for the corresponding complexes of the Mn-containing proteins. The high-pH Y34F Fe complex (Figure 7B) also appears to reflect six-coordination, while the significantly more axial character of

the EPR spectrum for the Fe derivative of the wt protein implies five-coordination in that case. In contrast to the six-coordinate complex reported for the high-pH form of authentic FeSD (Tierney et al., 1995), Fe_2-MnSD appears to retain five-coordination at high pH, converting to six-coordination on azide binding.

One of the key intermediates in $O_2^{\bullet -}$ dismutation is the peroxyanion formed by one-electron reduction of the superoxide radical that can be studied directly by examining the interaction of hydrogen peroxide with the enzyme. Transition metal−peroxide complexes are generally unstable toward O−O bond cleavage, forming hydroxyl radicals and higher oxidation state metal species, and efficient elimination of hydrogen peroxide must be an essential aspect of the catalytic mechanism of superoxide dismutase. In general, FeSD and Fe-substituted MnSD tend to be more sensitive to peroxide than their Mn-containing counterparts (Meier et al., 1994; Beyer & Fridovich, 1987; Yamakura & Suzuki, 1986), a trend that is also apparent here. Inactivation of FeSD by peroxide has been shown to result from oxidation of amino acid side chains [principally tryptophan (Yamakura, 1984; Beyer & Fridovich, 1987)] by a high-potential oxidant formed in the active site. The greater sensitivity of the Fe-substituted Y34F mutant (Figure 8) provides evidence implicating tyrosine-34 in peroxide interactions in the active site. Although transient oxidation of histidine ligands has been proposed as a mechanism for product inactivation of FeSD (Beyer & Fridovich, 1987), metal-centered oxidation and formation of oxo-Fe intermediates may be more likely, since both Fe and Mn enzymes share the same protein environment yet only Fe complexes undergo this reaction. The resistance of the Mn enzymes would then be a consequence of the distinct oxidation chemistries characteristic of Mn and Fe.

These results on anion binding and peroxide reactivity suggest a picture of product formation involving a transient hydroperoxide anion complex whose release depends on efficient delivery of a proton from the protein. The stability of the peroxide complex will depend on the Lewis basicity of the other metal ligands, which will assist in release of peroxide product in the final stroke of the turnover cycle. The hydroperoxide-labilizing proton may derive from the cluster of protons associated with Y34, Q146, and coordinated solvent, and the role of Tyr-34 in superoxide dismutation may be to maintain the appropriate protonation state of this proton cluster.

The significant catalytic activity of both wt and Y34F mutant Fe_2-MnSD is of special biological interest. While the activity of the Fe-substituted wt enzyme is significantly diminished below physiological pH (Figure 6), the mutant enzyme is active to relatively high pH (Figure 6) and its maximal activity is actually higher than that of wt Fe_2-MnSD at low pH, up to 20% of the activity of the Mn-containing enzyme. A number of "cambialistic" superoxide dismutases (Martin et al., 1986; Yamakura et al., 1991, 1995; Gabbianelli et al., 1995; Meier et al., 1995) have been isolated from anaerobic prokaryotes that function with either Mn or Fe in the active site. Mutagenesis of the gateway tyrosine residue in *E. coli* MnSD, which normally functions only with manganese, appears to relax the metal specificity and convert a selective enzyme into a relatively cambialistic one by altering the properties of the metal ligands in the relay pathway, which may be the key to determining metal selectivity in Fe and Mn superoxide dismutases. The observation that all cambialistic superoxide dismutases retain the conserved gateway tyrosine residue suggests that it may have an additional role in enzyme function.

CONCLUSIONS

The strictly conserved tyrosine at the gateway to the active site in all known Mn and Fe superoxide dismutases from bacteria to man functions in controlling the Lewis basicity of the anionic ligands (solvent hydroxide and aspartic carboxylate) of the redox-active Mn ion and therefore the coordination number and geometry of the metal complex. While Y34 phenolic hydroxyl is evidently not the immediate proton donor for superoxide dismutase turnover, it appears to be important for controlling anion interactions (including peroxide complexation and hydrolysis of the metal complex). The tyrosine is not essential for superoxide dismutase activity but contributes significantly to the catalytic rate enhancement of the enzyme, perhaps as much as 20% of the observed steady-state rate.

REFERENCES

Amano, A., Shizukuishi, S., Tsunemitsu, A., Maekawa, K., & Tsunasawa, S. (1990) *FEBS Lett. 272*, 217−220.

Baes, C. F., Jr., & Messmer, R. E. (1986) *The Hydrolysis of Metal Cations*, R. E. Kreiger Publishing Co., Malabar, FL.

Bannister, J. V., Bannister, W. H., & Rotilio, G. (1987) *CRC Crit. Rev. Biochem. 22*, 111−180.

Beyer, W. F., Jr., & Fridovich, I. (1987) *Biochemistry 26*, 1251−1257.

Beyer, W. F., Jr., & Fridovich, I. (1991) *J. Biol. Chem. 266*, 303−308.

Borgstahl, G. E., Parge, H. E., Hickey, M. J., Beyer, W. F., Jr., Hallewell, R. A., & Tainer, J. A. (1992) *Cell 71*, 107−118.

Borrello, S., De Leo, M. E., & Galeotti, T. (1993) *Mol. Aspects Med. 14*, 253−258.

Bravard, A., Sabatier, L., Hoffschir, F., Ricoul, M., Luccioni, C., & Dutrillaux, B. (1992) *Int. J. Cancer 51*, 476−480.

Bull, C., Niederhoffer, E. C., Yoshida, T., & Fee, J. A. (1991) *J. Am. Chem. Soc. 113*, 4069−4076.

Carlioz, A., & Touati, D. (1986) *EMBO J. 5*, 623−630.

Carlioz, A., Ludwig, M. L., Stallings, W. C., Fee, J. A., Steinman, H. M., & Touati, D. (1988) *J. Biol. Chem. 263*, 1555−1562.

Carter, P., & Wells, J. A. (1988) *Nature 332*, 564−568.

Church, S. L., Grant, J. W., Ridnour, L. A., Oberley, L. W., Swanson, P. E., Meltzer, P. S., Trent, J. M.; Cooper, J. B., McIntyre, K., Badasso, M. O., Wood, S. P., Zhang, Y., Garbe, T. R., & Young, D. (1995) *J. Mol. Biol. 246*, 531−544.

Deng, H. X., Hentati, A., Tainer, J. A., Iqbal, Z., Cayabyab, A., Hung, W. Y., Getzoff, E. D., Hu, P., Herzfeldt, B., Roos, R. P., Warner, C., Deng, G., Soriano, E., Smyth, C., Parge, H. E., Ahmed, A., Roses, A. D., Hallewell, R. A., Pericak-Vance, M. A., & Siddique. T. (1993) *Science 261*, 1047−1051.

Dingle, R. (1962) *J. Mol. Spectrosc. 9*, 426−427.

Dingle, R. (1965) *Inorg. Chem. 4*, 1287−1290.

Dingle, R. (1966) *Acta Chem. Scand. 20*, 33−44.

Everett, A. J., & Minkoff, G. J. (1953) *Trans. Faraday Soc. 49*, 410−414.

Farr, S. B., D'Ari, R., & Touati, D. (1986) *Proc. Natl. Acad. Sci. U.S.A. 83*, 8268−8272.

Fridovich, I. (1986) *Adv. Enzymol. Relat. Areas Mol. Biol. 58*, 61−97.

Fridovich, I. (1995) *Annu. Rev. Biochem. 64*, 97−112.

Gabbianelli, R., Battistoni, A., Polizio, F., Carri, M. T., De Martino, A., Meier, B., Desideri, A., & Rotilio, G. (1995) *Biochem. Biophys. Res. Commun. 216*, 841−847.

Goodin, D. B., & McRee, D. E. (1993) *Biochemistry 32*, 3313−3324.

Griffith, J. S. (1964) *Theory of Transition-Metal Ions*, Cambridge University Press, Cambridge, England.

Hassan, H. M. (1989) *Adv. Genet. 26*, 65−97.
Hsu, J. L., Hsieh, Y., Tu, C., O'Conner, D., Nick, H. S., & Silverman, D. N. (1996) *J. Biol. Chem. 271*, 17687−17691.
Keele, B. B., Jr., McCord, J. M., & Fridovich, I. (1970) *J. Biol. Chem. 245*, 6176−6181.
Keyer, K., Gort, A. S., & Imlay, J. A. (1995) *J. Bacteriol. 177*, 6782−6790.
Köhler, P., Massa, W., Reinen, D., Hofmann, B., & Hoppe, R. (1978) *Z. Anorg. Allg. Chem. 446*, 131−158.
Lah, M. S., Dixon, M. M., Pattridge, K. A., Stallings, W. C., Fee, J. A., & Ludwig, M. L. (1995) *Biochemistry 34*, 1646−1660.
Longo, V. D., Gralla, E. B., & Valentine, J. S. (1996) *J. Biol. Chem. 271*, 12275−12280.
Lowry, O. H., Rosebrough, N. J., Farr, A. L., & Randall, R. J. (1951) *J. Biol. Chem. 193*, 265−275.
Ludwig, M. L., Metzger, A. L., Pattridge, K. A., & Stallings, W. C. (1991) *J. Mol. Biol. 219*, 335−358.
Luft, R., & Landau, B. R. (1995) *J. Intern. Med. 238*, 405−421.
Martin, M. E., Byers, B. R., Olson, M. O., Salin, M. L., Arceneaux, J. E., & Tolbert, C. (1986) *J. Biol. Chem. 261*, 9361−9367.
McCord, J. M. (1976) *Adv. Exp. Med. Biol. 74*, 540−550.
McCord, J. M., & Fridovich, I. (1969) *J. Biol. Chem 244*, 6049−6055.
McCord, J. M., Boyle, J. A., Day, E. D., Jr., Rizzolo, L. J., & Salin, M. L. (1977) in *Superoxide and Superoxide Dismutases* (Michelson, A. M., McCord, J. M., & Fridovich, I., Eds.) pp 129−138, Academic, New York.
Meier, B., Sehn, A. P., Michel, C., & Saran, M. (1994) *Arch. Biochem. Biophys. 313*, 296−303.
Meier, B., Michel, C., Saran, M., Huttermann, J., Parak, F., & Rotilio, G. (1995) *Biochem. J. 310* (3), 945−950.
Meier, A. E., Whittaker, M. M., & Whittaker, J. W. (1996) *Biochemistry 35*, 348−360.
Nagano, S., Tanaka, M., Watanabe, Y., & Morishima, I. (1995) *Biochem. Biophys. Res. Commun. 207*, 417−423.
Nagano, S., Tanaka, M., Ishimori, K., Watanabe, Y., &Morishima, I. (1996) *Biochemistry 35*, 14251−14258.
Nagley, P., Mackay, I. R., Baumer, A., Maxwell, R. J., Vaillant, F., Wang, Z. X., Zhang, C., & Linnane, A. W. (1992) *Ann. N.Y. Acad. Sci. 673*, 92−102.
Parker, M. W., & Blake, C. C. (1988a) *FEBS Lett 229*, 377−382.
Parker, M. W., & Blake, C. C. (1988b) *J. Mol. Biol. 199*, 649−661.
Parker, M. W., Blake, C. C., Barra, D., Bossa, F., Schinina, M. E, Bannister, W. H., & Bannister, J. V. (1987) *Protein Eng 1*, 393−397.
Privalle, C. T., Beyer, W. F., Jr., & Fridovich, I. (1989) *J. Biol. Chem*. *264*, 2758−2763.
Roberts, V. A., Fisher, C. L., Redford, S. M., McRee, D. E., Parge, H. E., Getzoff, E.D., & Tainer, J. A. (1991) *Free Radic. Res. Commun. 12−13*, 269−278.
Satterlee, J. D., Alam, S. L., Mauro, J. M., Erman, J. E., & Poulos, T. L. (1994) *Eur. J. Biochem. 224*, 81−87.
Sawyer, D. T., & Valentine, J. S. (1981) *Acc. Chem. Res. 14*, 393−400.
Schapira, A. H. (1993) *Curr. Opin. Genet. Dev. 3*, 457−465.
Schmidt, M., Meier, B., & Parak, F. (1996) *J. Biol. Inorg. Chem. 1*, 532−541.
Slykehouse, T. O. and Fee, J. A. (1976) *J. Biol. Chem. 251*, 5472−5477.
Stallings, W. C., Metzger, A. L., Pattridge, K. A., Fee, J. A., & Ludwig, M. L. (1991) *Free Radic. Res. Commun. 12−13* (1), 259−268.
Stallings, W. C., Bull, C., Fee, J. A., Lah, M. S., & Ludwig, M. L. in *Molecular Biology of Free Radical Scavenging Systems* (Scandalios JG Ed) Cold Spring Harbor Lab Press, Plainview NY 1992
Stoddard, B. L., Howell, P. L., Ringe, D., & Petsko, G. A. (1990a) *Biochemistry 29*, 8885−8893.
Stoddard, B. L., Ringe, D., & Petsko, G. A. (1990b) *Protein Eng 4*, 113−119.
Tierney, D. L., Fee, J. A., & Penner-Hahn, J. E. (1995) *Biochemistry 34*, 1661−1668.
van Loon, A. P., Pesold-Hurt, B., & Schatz, G. (1986) *Proc. Natl. Acad. Sci. U.S.A. 83*, 3820−3824.
Weisiger, R. A., & Fridovich, I. (1973) *J. Biol. Chem. 248*, 4793−4796.
Whittaker, J. W. (1997) *J. Phys. Chem. B 101*, 674−677.
Whittaker, J. W., & Whittaker, M. M. (1991) *J. Am. Chem. Soc. 113*, 5528−5540.
Whittaker, M. M., & Whittaker, J. W. (1996) *Biochemistry 35*, 6762−6770.
Yamakura, F. (1984) *Biochem. Biophys. Res. Commun. 122*, 635−641.
Yamakura, F., & Suzuki, K. (1986) *Biochim. Biophys. Acta 874*, 23−29.
Yamakura, F., Matsumoto, T., & Terauchi, K. (1991) *Free Radic. Res. Commun. 12−13* (1), 329−334.
Yamakura, F., Matsumoto, T., & Kobayashi, K. (1994) in *Frontiers of Reactive Oxygen Species in Biology and Medicine* (Asada, K., & Yoshikawa, T., Eds.) pp 115−118, Elsevier Science B.V. Amsterdam.
Yamakura, F., Kobayashi, K., Ue, H., & Konno, M. (1995) *Eur J Biochem 227*, 700−706.
Yost, F. J., Jr., & Fridovich, I. (1976) *J. Biol. Chem. 248*, 4905−4908.
Youn, H.-D., Kim, E.-J., Roe, J.-H., Hah, Y. C., & Kang, S.-O. (1996) *Biochem. J. 318*, 889−896.

BI9704212